Proceedings of the ASME 2021 International Technical Conference and Exhibition on Packaging and Integration of Electronic and Photonic Microsystems
IPACK2021
October 27-29, 2021, online, USA

IPACK2021-74071 (Draft)

ADDITIVELY PRINTED FLEXIBLE TEMPERATURE SENSOR FOR WEARABLE APPLICATIONS

Pradeep Lall[1], Hyesoo Jang[1], Jinesh Narangaparambil[1], Kartik Goyal[1], Curtis Hill[2]

[1]Auburn University, NSF-CAVE3 Electronics Research Center, Auburn, AL 36849
[2]QuantiTech Inc, Jacobs Space Exploration Group, ESSCA Contract, NASA MSFC
Tele: +1(334)844-3424; E-mail: lall@auburn.edu

ABSTRACT

The flexible sensor has the capability to be mounted on any curved surfaces of applications and be used for portable devices. Additively printed sensors have received attention owing to their compact design and ability of application to non-planar surfaces. Wearable applications require capability of integration into a variety of surfaces with ability to flex, fold, twist and stretch under the stresses of daily motion. There is scarcity of data on the interaction of the process parameters with the realized performance. In addition, there is need for data focused on sensor accuracy, repeatability, and reliability. In this study, experimental analysis on function of the fabricated sensing board is conducted. The temperature sensors are made by direct write printing method with nScrypt printer. A calibration of the sensors has been conducted to confirm that resistance is well related to actual temperature and find TCR (temperature coefficient to resistance). The evolution of resistance has been correlated with the environmental temperature. The sensor hysteresis has been quantified using upswing and downswing of the environmental temperature. In addition, the effect of humidity on the temperature sensor accuracy and performance has been quantified. The effect of a polymide coat on the sensor to prevent humidity effects has also been quantified.

Keywords: Printed Electronics, Temperature Sensor, Prognostics and Health Monitoring, Reliability of Devices, Reliability Modelling and Simulation, Reliability Test Methods.

1. INTRODUCTION

Flexible hybrid electronics has gained a lot of attention owing to performance benefits such as flexibility, lightweight and compactness. A number of environmental monitoring application have become possible owing to the emergence of additive flexible print processes. Examples include temperature and humidity monitoring. However, the accuracy, repeatability and reliability of the sensor performance or process-performance interaction has not been quantified for the additive print processes. Wearable applications require the integration of sensors into form-factors capable of folding, flexing and twisting under the stresses of daily motion. Wearable temperature sensors can be used to sense environmental temperature extremes and body temperature in performance applications for health monitoring. Temperature may be measured through measurement of the change in resistance with the change in temperature.

Sensor inks may decrease in resistance with the increase in temperature indicating a negative temperature coefficient of resistance (NTC) or increase in resistance with the increase in temperature indicating a positive temperature coefficient of resistance (PTC). In general, NTC materials demonstrate a more non-linear curve of resistance vs temperature than that of a PTC material. A number of metallic inks demonstrate a positive temperature coefficient of resistance. However, there are efforts of cost-effective fabrication of PTC type sensor with silicon-based materials such like PDMS (polyimethylsiloxane) [Wang 2019]. Owing to the need of a small form-factor in wearables, PTC type sensors may be better choice because the non-linearity of NTC type needs multi-point calibration and additional circuit for compensation of the non-linearity. For additive printed electronics, inkjet printing, direct-write, screen printing, and aerosol jet print printing methods are widely used.

Figure 1 shows the schematic of sensing mechanism of temperature sensor with a PTC or a NTC material. The resistance of the PTC and NTC materials is changed while the ambient temperature is changed as shown on equation (1):

$$R = R_0[1 + \alpha(T - T_0)]$$
$$where,\ R: resistance, R_0: initial\ resistance$$
$$\alpha: \text{temperature coefficient of resistance (TCR)},$$
$$T: temperature\ (\text{K}), T_0 = 293\ (\text{K}) \quad (1)$$

The *resistance* (R) is proportional to *temperature coefficient of resistance* $(TCR, \alpha) \times temperture\ (T)$, where TCR is dependent on material properties and needed to be stable for

[1] Contact author: lall@auburn.edu

Table I: State of the art

Type	Substrate	Electrode	Sensitive materials	Method	T. range (°C)	TCR (%/°C)	Reference
PTC	Paper	Ag	Ag	Inkjet	-20 to 60	0.11	Courbat 2011
NTC	PEN	Ag	CNT +PEDOT:PSS	Inkjet	20 to 70	-0.25	Bali 2016
NTC	PET	Ag	CNT	Screen	-40 to 100	-0.40	Turkani 2018
PTC	Silicon	-	GO+PDMS	D-write	25 o 75	0.8	Wang 2019
NTC	Silk+ Glass	PEDOT:PSS	rGO	UVL	20 to 50	-0.99	Pradhan 2020
NTC	PI	Ag	GO+PEDOT:PSS	UVL	25 to 100	-1.09	Soni 2020
NTC	PDMS	Ag	rGO+PHB	Inkjet	20 to 60	1.8	Dan 2020
PTC NTC NTC	PI	Ag	Ag CNT PEDOT:PSS	Screen	-20 to 120	0.21 -0.05 -0.07	Lall 2020

TCR = (R– Rref)/Rref (T–Tref) where $T_{ref} = 20℃$, PTC: positive temperature coefficient, NTC: negative temperature coefficient, PEN: Polyethylene naphthalate, CNT: Carbon nanotube, PEDOT:PSS: poly(3,4-ethylenedioxythiophene) polystyrene sulfonate, PET: Polyehyleneterephthalate, PDMS: polyimethylsiloxane, rGO: reduced graphene oxide, UVL: ultraviolet lithography, PI: Polyimide, PHB: Polyhydroxybutyrate, D-write: Direct writing

sensing a wide range of temperature. The resistance of PTC is increased by increased temperature because TCR is positive. In the case of NTC materials, such relationship is reversed because the TCR is negative. There is previous research on the printed temperature sensor with various materials for the printing ink and substrate in different printing method as shown on the Table I. Throughout the table, TCR in specific range of temperature could be easily compared.

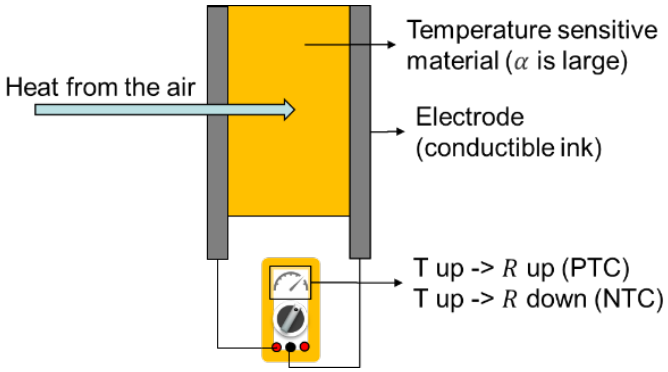

Figure 1: Schematic of temperature sensor

A sensitive sensor material should have low hysteresis and low correlation with humidity and strain for accuracy of temperature measurement. For the low hysteresis, the property of sensitive material is significant. For the low relationship between resistance and humidity, an encapsulation of the sensitive materials might be helpful. But the encapsulation might prevent heat transfer from the air to the sensitive materials so that it could delay the resistance change of the material and in turn, hysteresis could be increased. In this regard, a material of encapsulation should have high heat conductivity and low porosity which could be transmitted by the humidity. Even as perspective of reliability of sensor, the encapsulation is needed.

Single layer additive printed sensors could be susceptible to the stresses because the traces are directly exposed to the air, thus delaminated from the substrate of the sensor. In this regard, it is assumed that the multi-layer traces with coat make the traces more resilient against the delamination due to the stresses. Additionally, multi-layer print method is essential for fabrication of complex printed temperature sensor such like vital sign acquisition system board for wearable device. The printed temperature sensor needs to have several via, interconnection, dielectric for integration of sensors on small PCB so that the board needs to be printed by multi-layer method Accordingly, there is growing need for development of resilient additive printing method. When the printed temperature sensor is exerted by the flex-stresses, the printed temperature sensor could be damaged. But size of the damage is judged by several factors such like process parameters of print, sintering temperature of post treatment of print, thickness of the substrate, etc. In these regards, the reliability test for printed temperature sensor would be needed.

In this study, the multilayer additive printed temperature sensor with various encapsulation method is fabricated for improved reliability of robustness on the flex-stresses, and humidity resistance. Two temperature sensors with 1-layer and 2-layers respectively are printed. A resistance variation of the sensors with respect to temperature and humidity was measured and TCR, which is linear regression analysis at 20-60°C was computed. Additionally, a resistance variation with respect to humidity with PI-coat (tape or encapsulation) was compared to such that without PI-coat. Quantification of delay time of temperature sensor w/wo PI coat on the circuits with respect to temperature variation has been measured and compared. Comparison study with resistance response of the sensors w/wo PI-coat was conducted to quantify the degradation of the response due to interruption of heat transfer because of PI coated

layer. Lastly, sensor accuracy was computed with several factors which are hysteresis, repeatability, nonlinearity and stability to find the best way of printing method.

2. TEST SETUP

Figure 2 shows additive printer with direct-write method by nScrypt and smart pump for ink direct-write. The print speed is 3mm/s, nozzle diameter of outside and inside is respectively, 159.1 and 244 μm. The heights of nozzle tip from substrate are 0.1 mm for first layer and 0.125 mm for second layer of active material of the sensors. An air pressure is 25 psi, and ink temperature is at 25℃. Once the circuits are printed, the sensor is cured by thermal oven in 15 min at 120℃.

Figure 2: Additive printer with direct write method by nScript (left) and smart pump for jet of ink (right)

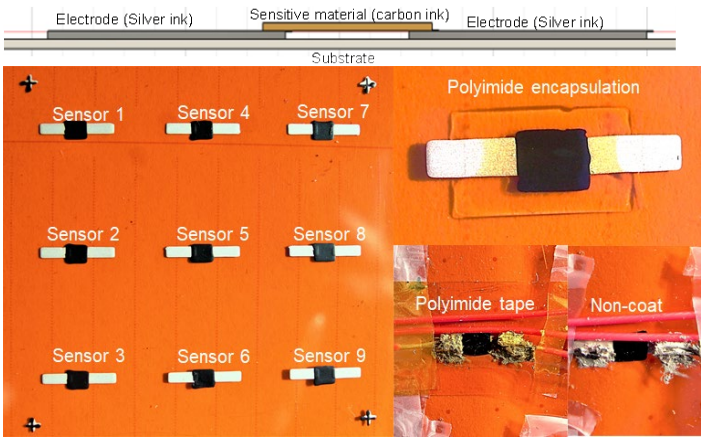

Figure 3: Multi-layered printed temperature sensors w/wo polyimide encapsulation and polyimide tape.

Figure 3 shows the printed temperature sensor, which is printed by direct-write method with CNT (carbon nanotube) ink for active material and silver paste ink for conductive traces. The material properties of the ink are shown on the Table II. The Table III presents the process parameter for the fabrication process of the multi-layered sample, which is developed by CAVE3 research center. Figure 4 portrays DAQ (data acquisition) system including the data logger, connected temperature sensor, humidifying and thermal chamber, and DAQ software. On the experiments, the resistance with respect to the temperature and humidity variation were acquired by the DAQ to compute the TCR and study effects of the humidity. To shorten the humidity effect, several encapsulations was assessed and compared side by side. Sensor response was quantified to see reliability of the sensor and adverse effect of encapsulations on the response time. Each test about humidity effect and the response time are compared by the sensors with PI tape and the sensors without PI tape.

Figure 4: Data acquisition system

Table II: Properties of inks [Dupont 2014] for direct write printing

List	Value	Unit
Viscosity	15-70	Pa·s
Operating temp	<80	℃
Designed resistance	~15	KΩ/□

Table III: Process parameters for printing the temperature sensors

List	1-layer	2-layer
Curing time (min)	15	10/15/20
Curing temperature (℃)	120	120/130
Print speed (mm/s)	3	3
Nozzle Dia. Out / in (μm)	159.1/244	159.1/244
Height of nozzle tip from substrate (mm)	0.1	0.1/0.125
Air pressure (psi)	25	25
Ink temperature (℃)	25	25

3. EXPERIMENTAL RESULTS

3.1 Measurement of resistance variation with respect to temperature

The sensor resistance has been measured and analyzed. Table IV shows initial resistance of the 1-layered and 2-layered sensors. As shown on the table, the initial resistance is increased with increment of the number of layers of printing traces because the thickness of the traces is increased. The quantity of the increment of the resistance seems not direct proportional to the number of layers because it might be assumed that final thickness of the traces becomes not doubled after the sintering process, which bind the particles of the ink so that the line is robust, and so that gaps of the particles are shrunk, which might result in decrement of the final thickness.

Figure 5 shows resistance variation versus temperature variation of various temperature sensors, which are 1-layered sensor, 2-layered sensor and encapsulated 2-layered sensor, respectively from top to bottom, with equivalent process recipe. As seen on the graphs, in a range of temperature from 20℃ to 60℃, 1-layered sensor is most sensitive while 2-layered sensor is relatively obtuse. Additionally, the encapsulated 2-layered sensor are most obtuse. Those results might from the TCRs of each sensor are computed by using equation (2) and those are, as shown on the Table V, 4.11, 3.47, 3.63, 3.71, 3.50, 3.75, 3.41 and 3.53 (%/℃) which have 0.0022 of standard deviation and 5.00×10^{-6} of variance. On the manufacturing process of encapsulated sensor, it is observed that the initial resistance of the sensor is soared to 10 times the initial resistance of 2-layered sample without the encapsulation after 2 minutes of thermal sintering of PI ink at 120℃. That might be because the polyimide is low conductive material and it is mixed up with the carbon particles, thus the resistance of active material is increased. Now that such process is chemical reaction, the TCR of the encapsulated sensor is varied sensor to sensor. In this regard, additional test might be needed to optimize the process parameters which could affect initial resistance and TCR.

$$\boldsymbol{R = R0[1 + \alpha(T - T0)]} \quad (2)$$

Table IV: Initial resistance of the 1-layered and 2-layered sensors

Initial resistance (KΩ)									
No.	**1**	**2**	**3**	**4**	**5**	**6**	**7**	**8**	**9**
1 layer	4.4	4.1	4.5	4.0	4.8	4.4	3.9	4.3	4.4
2 layers	2.9	3.2	3.3	2.9	3.0	3.1	2.9	3.0	3.2

Table V: TCR from 60℃ to 80℃

TCR (%/℃) from 60℃ to 80℃									
No.	**1**	**2**	**3**	**4**	**5**	**6**	**7**	**8**	**9**
1 layer	4.1	3.5	3.6	3.7	3.5	-	3.8	3.4	3.5
2 layers	3.1	3.8	3.9	3.2	3.7	4.0	3.3	4.3	4.3
2 layers PI Encap'	4.9	1.2	-	-	2.3	-	12.8	4.1	-

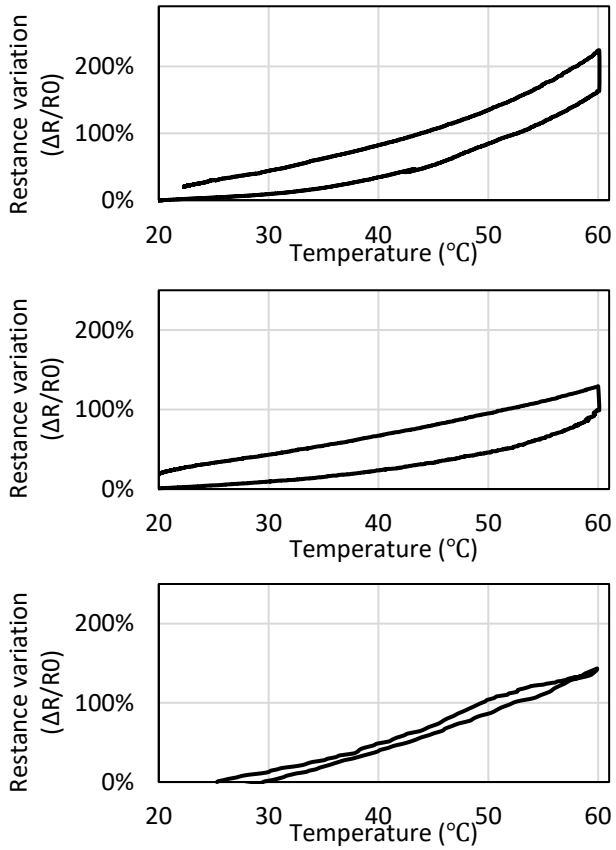

Figure 5: Resistance variation versus temperature variation of various temperature sensors, which are 1-layered sensor, 2-layered sensor and encapsulated 2-layered sensor, respectively from top to bottom, with equivalent process recipe.

3.2 Responsiveness test on the resistance of the sensors with respect to rapid variation of temperature

Resistance response to temperature variation of the temperature sensor might depend on heat capacity of the active material of the sensor and heat transfer. To shorten the response time, the heat capacity should be low, and the heat transfer is high. In this research, it might be observed that the number of the layer and coat material is not significantly, affecting on the response time. Figure 6 shows resistance variation and its rate on rapid temperature variation from 25℃ to 40℃ and it seems that the resistance variation rate is analogous to sensor to sensor. The response of the sensors itself is fast within a minute at most, while the equilibrium time is quite long to take few minutes. That is because the carbon ink has larger heat capacity as compared to metallic materials such as Ag, Pt, etc. But the metallic material is not cost effective and might suffer from too sensitiveness (i.e. self-heating issue or being affected by resistance of electrode). Figure 7 shows resistance variation rate (ΔR/min) of one-layered temperature sensors with respect to the rapid temperature change at 25-40℃, 40-60℃ and 60-80℃, respectively, from top to bottom. As shown on the Figure 3, the PI tape is attached on the sensors to enhance mechanical viability and humid reliability. The thing is that if the PI layer is added, the heat transfer might

be degraded so that the response of the sensors might be delayed. As seen on the graphs, there were no significant delay which arise from the PI layer on the contrary to such expectations.

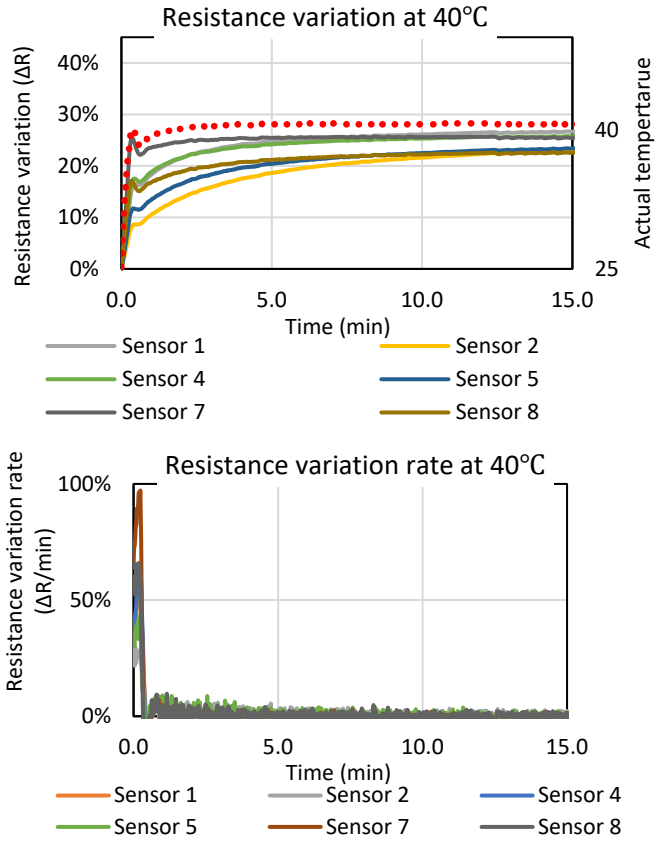

Figure 6: Resistance variation and its rate on rapid temperature variation from 25℃ to 40℃

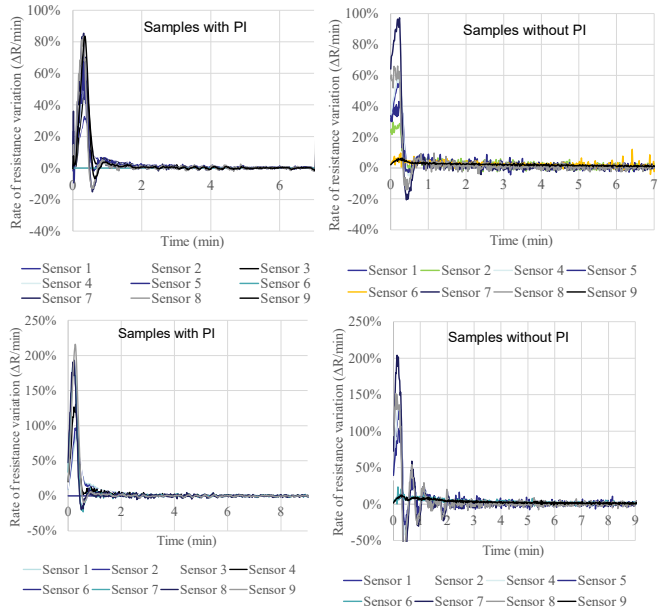

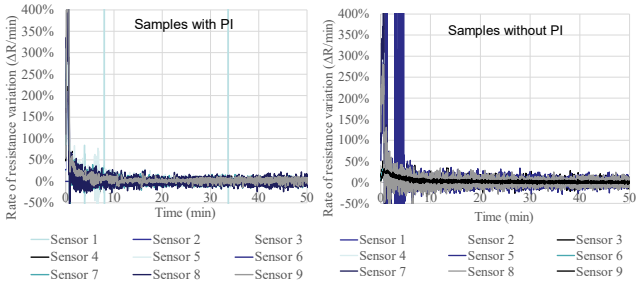

Figure 7: Resistance variation rate (ΔR/min) of one-layered temperature sensor with respect to the rapid temperature change at 25-40℃, 40-60℃ and 60-80℃, respectively, from top to bottom.

3.3 Humid reliability of the sensors with respect to variation of relative humidity

Carbon material is porous material and it might absorb moisture from environment especially on the situation in high temperature and relative humidity. The absorption of moisture could make the active material more resistive to current conduction, thus the sensor could have error on sensing temperature. For the humid-reliability of the temperature sensor with respect to variation of relative humidity, surface coat such as encapsulation, laminate, additional layer, etc. might be needed. Figure 8 shows resistance variation (ΔR/R0) of one-layered temperature sensor with respect to the humidity. The Sensor 4, 7 and 8 has one, two and three layers of PI tape, respectively and compared sensor has no PI tape. The graphs are comparing to see an effect of PI tape about prevention of humidity. As shown on the graphs, at 25℃, the difference is tiny by 1% so that the characteristics between the variation rate w/wo PI tape seems similar each other.

Figure 9 shows resistance variation of one-layered temperature sensor with respect to the humidity at 40℃. The first graph is about sensor with no coat on its surface while on the second graph, Sensor 4, 7 and 8 has one, two and three layers of PI tape, respectively. On the last graph, the sensor is encapsulated with PI ink and sintered. As shown on the graph, non-coated sample has most high resistance variation by around 23% with respect to relative humidity from 10 % to 70 % while the sample with PI tape has around 18% of resistance variation. It is assumed that the encapsulated sensor has best quality of humid-reliability, which has 10% to 18 % of resistance variation.

Figure 10 shows resistance variation of the sensors versus the humidity at 80℃. The status of the sensors is same with previous paragraph. As shown on the first graph, the resistance variation of non-coated sensor is huge by 90%, while on the second graph, the sensors with PI tape have only 30% of resistance variation. On the last graph, PI-encapsulated sensor has lowest resistance variation by 10% at most. Additionally, an effect of the number of layers of PI tape seems not relevant to the resistance variation in the range of this study.

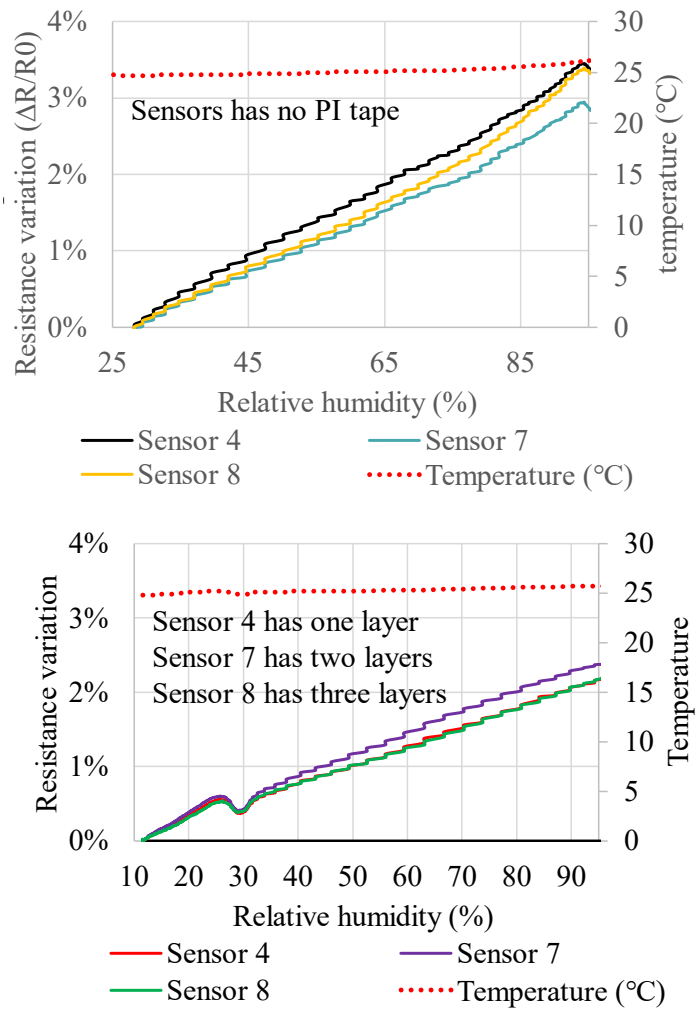

Figure 8: Resistance variation (Ω/R0) of one-layered temperature sensor with respect to the humidity at 25°C.

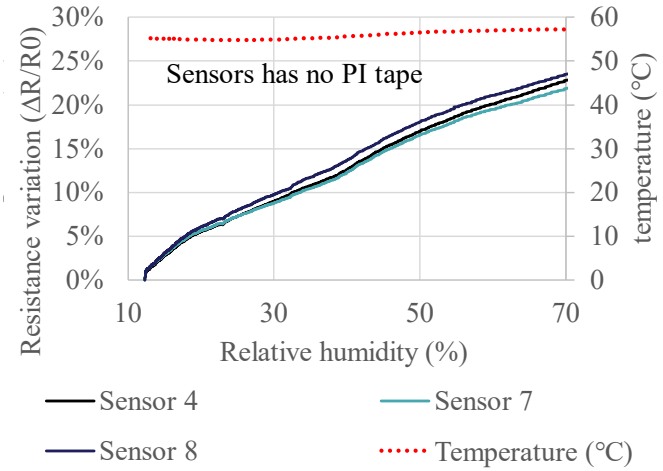

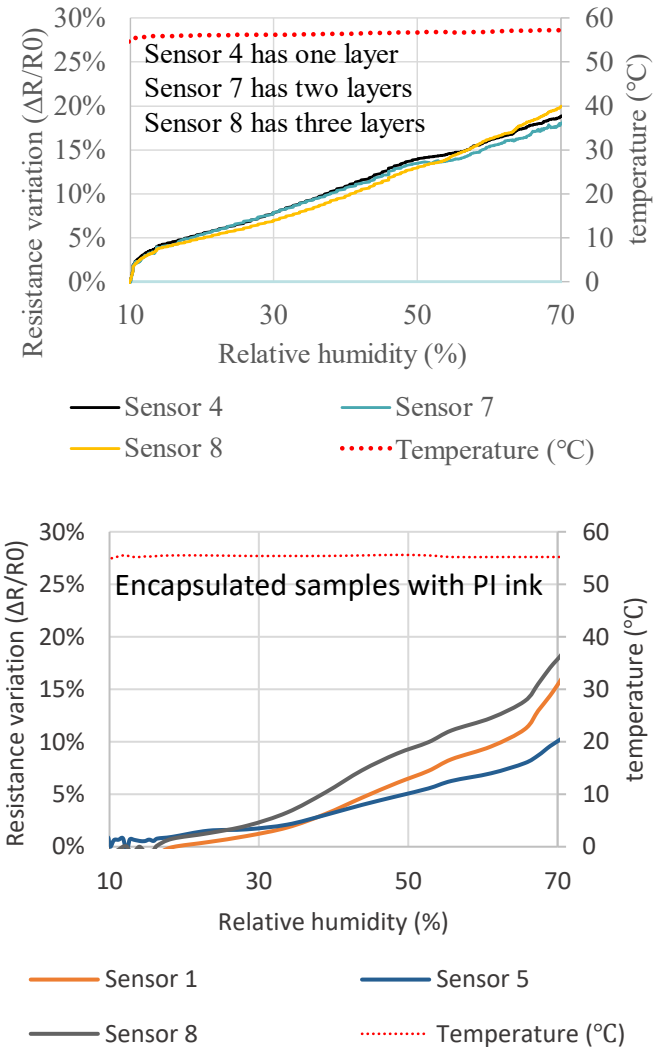

Figure 9: Resistance variation (Ω/R0) of one-layered temperature sensor with respect to the humidity at 40°C.

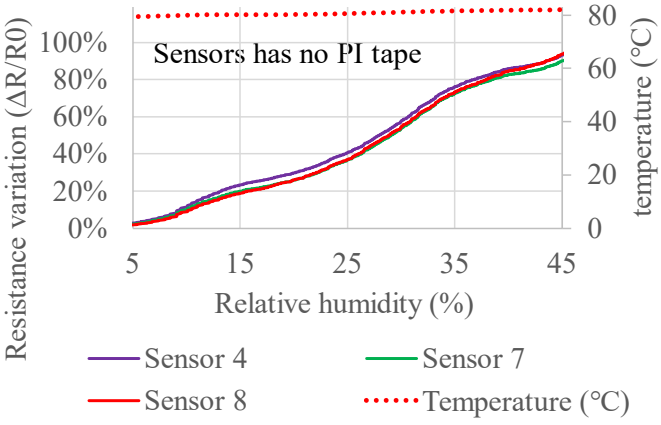

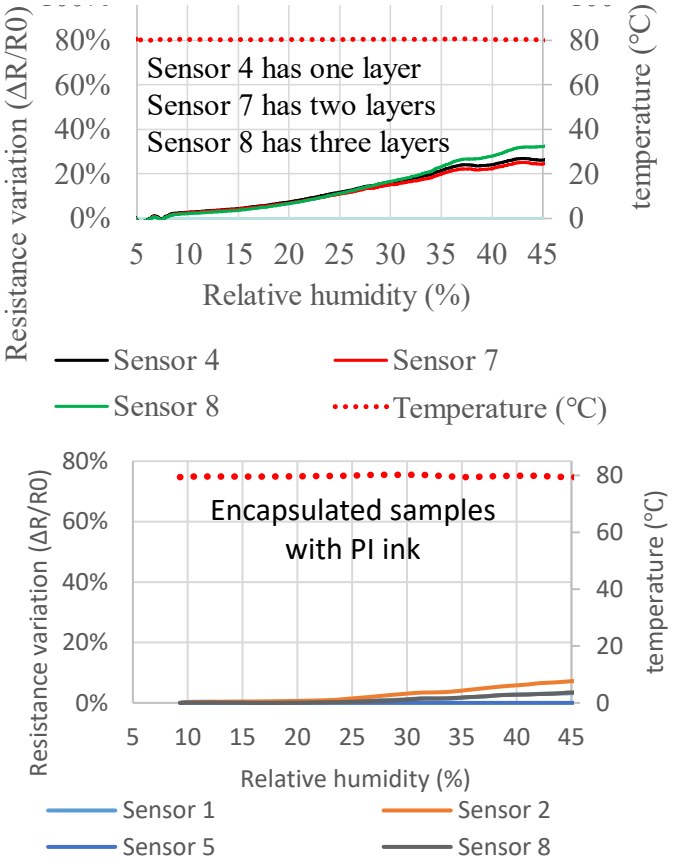

Figure 10: Resistance variation (Ω/R0) of one-layered temperature sensor with respect to the humidity at 80℃.

3.4 Sensor accuracy with repeatability, hysteresis, nonlinearity and long-term stability

In this section, sensor accuracy was computed by the equations (3-6). As shown on the equation (3), the sensor accuracy hysteresis, non-linearity, repeatability and stability. Figure 11 shows computation method of the hysteresis of the sensors, where the hysteresis is computed by difference among the maximum resistance variation of downsweep, and resistance variation of upsweep. Figure 12 shows Computation of the nonlinearity which is computed by difference among the maximum resistance variation of linear line on both terminal points from started point to finished point of measurement, and resistance variation of measurements. Equation (6) shows the non-repeatability which is coefficient of pooled variation of the measured resistance, recursively with respect to the specific temperature points and Table VI portrays an example of the computation of it. Table VII presents the results of the sensor accuracy of the samples. As shown on the table, there was no significant relation among the number of layers and the sensor accuracy while the encapsulation is significantly affecting on the sensor accuracy. With a consideration of humid reliability and sensor accuracy, encapsulated sensor seems best way of the printing, but the unstable TCR and high initial resistance might be an outstanding issue hereafter.

$$\textbf{Sensor accuracy} = \sqrt{\frac{(\textbf{Hysteresis})^2+(\textbf{Non linearity})^2+(\textbf{Non repeatability})^2+(\textbf{Stability})^2}{4}} \quad (3)$$

$$\textbf{Hysteresis} = \textbf{Max}(R_{downsweep} - R_{upsweep}) \quad (4)$$

$$\textbf{Nonlinearity}\ (\%) = \textbf{Max}(R_{TP} - R_{measurement}) \quad (5)$$

$$\textbf{Non-repeatability}\ (\%) = \frac{\sqrt{\frac{\sum v_i \cdot s2_{1i}}{\sum v_i}}}{\mu} \quad (6)$$

Where, μ_i = mean, S_{1i} = Standard deviation, v_i = Degrees of freedom

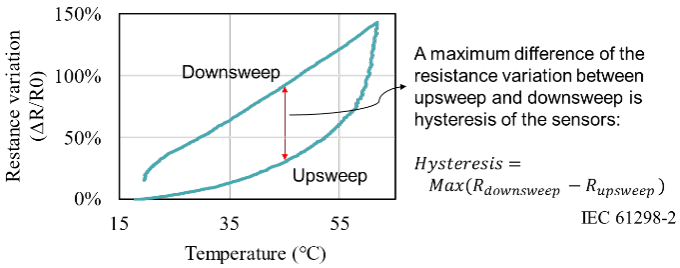

Figure 11: Computation of the hysteresis of the samples

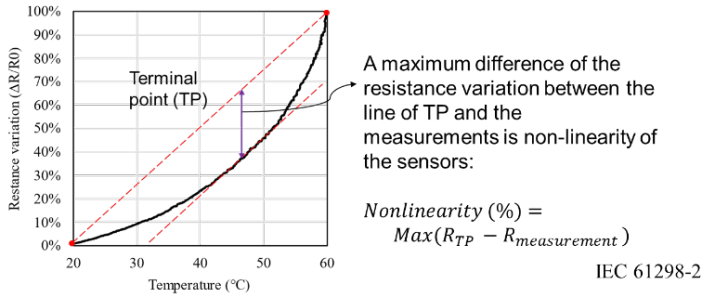

Figure 12: Computation of the nonlinearity of the samples

Table VI: Computation of the repeatability of the samples

	REPEATABILITY TEST						
	Test #\Temp(℃)	**25**	**30**	**35**	**40**	**55**	**60**
Expression	1 (Ω)	4,105	4,361	4,873	5,648	8,707	10,662
	2 (Ω)	3,447	3,570	3,793	4,145	6,671	7,908
	3 (Ω)	-	4,470	3,596	5,219	5,121	7,159
μ_i	MEAN	3,776	4,134	4,087	5,004	6,833	8,576
S_{1i}	Standard deviation (SD)	466	491	688	775	1,799	1,845
v_i	Degrees of freedom (DOF)	1	2	2	2	2	2
$SS_i = v_i \cdot S_{1i}$	Weighted variance - Sum of squares (SS)	2.2 E5	4.8 E5	9.5 E5	1.2 E6	6.5 E6	6.8 E6

	REPEATABILITY TEST	
$ESS = \sum SS_i$	Total weighted variance - total sum of squares (ESS)	16,120,954
$\nu = \sum v_i$	Total degrees of freedom (EDOF)	11
$Sp = \sqrt{ESS/\nu}$	Pooled standard deviation (Sp)	1,211
Sp/μ	Standard non-repeatability (%)	24%

Table VII: Sensor accuracy of the samples

One-layered sample									
Sensor No.	1	2	3	4	5	6	7	8	9
Hysteresis (%)	38	39	44	36	38	-	34	34	37
Non-linearity (%)	29	29	31	29	29	-	29	29	29
Non-repeatability (%)	18	18	24	16	19	-	17	17	22
Stability (%)	1	33	1	0	0	-	0	0	1
Accuracy (RMS %)	36.2	43.2	41.5	34.6	36.3	-	33.7	33.9	36.7
Two-layered sample									
Hysteresis (%)	36	25	24	44	29	-	48	28	24
Non-linearity (%)	31	29	29	33	31	-	34	31	30
Non-repeatability (%)	24	23	23	23	24	-	22	22	21
Stability (%)	4	26	2	3	7	-	3	6	3
Accuracy (RMS %)	38.1	36.3	31.2	41.9	34.4	-	44.6	33.6	30.8
Encapsulated and two-layered sample									
Hysteresis (%)	15	11	-	-	13	-	17	14	-
Non-linearity (%)	7	17	-	-	8	-	21	10	-
Non-repeatability (%)	11	6	-	-	8	-	19	19	-
Accuracy (RMS %)	14.1	14.9	-	-	12.1	-	23.2	18.2	-

4. SUMMARY AND CONCLUSIONS

In this study, the multilayer additive printed temperature sensors w/wo polyimide coats with different method are fabricated for improved reliability of robustness on flex-stresses, humid reliability and sensor accuracy. The characteristics of the temperature sensor was studied, and it is found that resistance is linearly related to temperature and related to humidity but the effect of it could be reduced with PI-coat. Especially, PI-encapsulated sensors have superb humid reliability as well as great sensor accuracy. On the contrary of initial expectation, the delay time of samples with PI tape is analogous to that of samples without PI tape. If the sensor accuracy and the humid reliability are preferred, the encapsulated sensor would be best choice, but there are remaining issue which related to the unstable TCR and high initial resistance. This paper has not enough test data to resolve the issues, thus additional research might be needed with extra process parameters and test conditions such as CT scan, SEM analysis, weight gain of moisture, etc.

ACKNOWLEDGEMENTS

The project was sponsored by the NASA (National Aeronautics and Space Administration) at the NSF-CAVE3 Electronics Research Center at Auburn University.

REFERENCES

1. Bali, C., Brandlmaier, A., Ganster, A., Raab, O., Zapf, J., & Hübler, A. "Fully inkjet-printed flexible temperature sensors based on carbon and PEDOT: PSS." Materials Today: Proceedings, 3(3), 739-745. (2016)
2. Courbat, J., Kim, Y. B., Briand, D., & De Rooij, N. F. "Inkjet printing on paper for the realization of humidity and temperature sensors." In 2011 16th International Solid-State Sensors, Actuators and Microsystems Conference (pp. 1356-1359). IEEE. 2011
3. Dan, L., & Elias, A. L. "Flexible and Stretchable Temperature Sensors Fabricated Using Solution-Processable Conductive Polymer Composites." Advanced Healthcare Materials, 9(16), 2000380. 2020
4. Lall, P., Goyal, K., & Narangaparambil, J. Accuracy, "Hysteresis and Extended Time Stability of Additively Printed Temperature and Humidity Sensors." In 2020 IEEE 70th Electronic Components and Technology Conference (ECTC) (pp. 1070-1080). IEEE. 2020
5. Pradhan, Sayantan, and Vamsi K. Yadavalli. "Photolithographically Printed Flexible Silk/PEDOT: PSS Temperature Sensors." ACS Applied Electronic Materials. 2020.
6. Serway, Raymond A., Clement J. Moses, and Curt A. Moyer. "Modern physics." Cengage Learning, 2004.
7. Soni, M., Bhattacharjee, M., Ntagios, M., & Dahiya, R. "Printed temperature sensor based on PEDOT: PSS-graphene oxide composite." IEEE Sensors Journal, 20(14), 7525-7531. 2020
8. Turkani, V. S., Maddipatla, D., Narakathu, B. B., Bazuin, B. J., & Atashbar, M. Z. "A carbon nanotube based NTC thermistor using additive print manufacturing processes." Sensors and Actuators A: Physical, 279, 1-9. 2018
9. Wang, Z., Gao, W., Zhang, Q., Zheng, K., Xu, J., Xu, W., ... & Liu, Y. "3D-printed graphene/polydimethylsiloxane composites for stretchable and strain-insensitive temperature sensors." ACS applied materials & interfaces, 11(1), 1344-1352. 2018
10. Dupont corp., "Technical Data Sheet of Dupont 7292 PTC Carbon Resistor", from https://www.dupont.com/content/dam/dupont/amer/us/en/products/ei-transformation/documents/7292.pdf, 2014